Available online at BCREC website: https://bcrec.id

Bulletin of Chemical Reaction Engineering & Catalysis, 17 (3) 2022, 650-660

Research Article

Synthesis of ZnO-Fe_3O_4 Magnetic Nanocomposites through Sonochemical Methods for Methylene Blue Degradation

Nanda Saridewi[1*], Sri Komala[2], Agustino Zulys[3], Siti Nurbayti[2], Latifah Tulhusna[4], A. Adawiah[5]

[1]*Department of Chemistry Education, Faculty of Tarbiya and Teaching Sciences, UIN Syarif Hidayatullah Jakarta, Jl. Ir. H. Juanda No. 95, Ciputat, South Tangerang 15412, Indonesia*
[2]*Department of Chemistry, Faculty of Science and Technology UIN Syarif Hidayatullah Jakarta , Jl. Ir. H. Juanda No. 95, Ciputat, South Tangerang 15412, Indonesia*
[3]*Department of Chemistry, Faculty of Mathematics and Natural Sciences, University of Indonesia, Jl. Lingkar Kampus Raya, Pondok Cina, Beji, Depok, West Java 16424, Indonesia*
[4]*Department of Public Health, Faculty of Health Science, UIN Syarif Hidayatullah Jakarta Jl. Kertamukti No. 5, Ciputat, South Tangerang, Banten 15412, Indonesia*
[5]*Integrated Laboratory Centre, Faculty of Science and Technology UIN Syarif Hidayatullah Jakarta, Jl. Ir. H. Juanda No. 95, Ciputat, South Tangerang 15412, Indonesia*

Received: 13rd August 2022; Revised: 15th September 2022; Accepted: 15th September 2022
Available online: 18th September 2022; Published regularly: September 2022

Abstract

Textile industry waste can pollute the aquatic environment because it contains dye contaminants with very stable properties that are difficult to degrade naturally. However, dye contaminants degradation can be carried out by photodegradation using ZnO-Fe_3O_4 magnetic nanocomposite photocatalysts. This study aims to synthesize ZnO-Fe_3O_4 magnetic nanocomposite through a sonochemical method. Then measure their photocatalytic activity in methylene blue degradation. The best ZnO-Fe_3O_4 magnetic nanocomposite is made of ZnO:Fe_3O_4 mass ratio of 4:1 with a crystal size of 31.058 nm, a hexagonal crystal phase and a particle size of 173.23 nm. The ZnO-Fe_3O_4 magnetic nanocomposites (4:1) provides optimum degradation capacity of methylene blue under halogen lamp irradiation of 99.56 mg/g at pH 13. Furthermore, the ZnO-Fe_3O_4 magnetic nanocomposites had good stability in 10 cycles reaction with a degradation capacity of 99.24-99.75 mg/g. The photocatalytic degradation of methylene blue by ZnO-Fe_3O_4 occurs through the formation of free radical species with hydroxyl radicals as the dominant species that play an important role in the degradation process.

Keywords: ZnO-Fe_3O_4; magnetic nanocomposite; degradation; photocatalysts; methylene blue

How to Cite: N. Saridewi, S. Komala, A. Zulys, S. Nurbayti, L. Tulhusna A. Adawiah, (2022) Synthesis of ZnO-Fe_3O_4 Magnetic Nanocomposites through Sonochemical Methods for Methylene Blue Degradation. *Bulletin of Chemical Reaction Engineering & Catalysis*, 17(3), 650-660 (doi: 10.9767/bcrec.17.3.15492.650-660)

Permalink/DOI: https://doi.org/10.9767/bcrec.17.3.15492.650-660

1. Introduction

The textile industry is one of the most significant contributors to water waste, that is declining water quality in the environment [1]. Dye waste produced by industry is generally non-biodegradable organic compounds, making them challenging to degrade [2]. One common dye types commonly produced by the textile industry is methylene blue [1].

Photocatalysis is a process of combination of photochemistry and catalyst. The photocatalysis begins with forming an excited electron on the conduction band and leaves an electron hole in

* Corresponding Author.
Email: nanda.saridewi@uinjkt.ac.id (N. Saridewi)

the valence band. Paired electron holes undergo an oxidation-reduction reaction producing free radicals (OH^*) that can degrade a harmful organic pollutant [3]. ZnO, an environmentally friendly photocatalyst [4], has unique properties: high chemical stability, good electrical properties, high light transmittance, and low price [5]. In addition, ZnO has a band gap of 3.37 eV [6-7]. Raganata *et al*. reported that ZnO nanoparticles can degrade methylene blue with degradation increasing as the irradiation time increases [8].

However, ZnO in water tends to form colloids, thus in the photodegradation process, it will reduce its degradation efficiency [9]. Therefore, ZnO photocatalytic activity can be optimized by developing a supporting material, such as is by composting using Fe_3O_4 material [10]. Furthermore, Fe_3O_4 has good chemical stability and does not agglomerate over a long time. In addition, the magnetic properties of Fe_3O_4 facilitates the ZnO-Fe_3O_4 nanocomposite separation process after being used in the liquid waste treatment. Therefore, photocatalysts can be reused continuously in the long term [12].

Many researchers have successfully synthesized ZnO-Fe_3O_4 nanocomposites using various methods. Ulya & Taufiq have successfully synthesized ZnO/Fe_3O_4 nanocomposites using sonochemical methods [13]. Yogasundari & Manikan reported that the Fe_3O_4-ZnO composite has been successfully synthesized through the coprecipitation method [14]. Ghanbarnezhad *et al*. reported that nanocomposites reduced graphene oxide (RGO)/Fe_3O_4-ZnO via the hydrothermal method [15]. Winatapura *et al*. fabricated Fe_3O_4-ZnO nanocomposites using a simple wet grinding method for methylene blue photodegradation [16]. Elshypany *et al*. synthesized Fe_3O_4/ZnO nanocomposites with a degradation efficiency against methylene blue of 88.5% with high stability of 5 reaction cycles [17]. Habibi & Shekofteh also synthesized Fe_3O_4-ZnO composites through the coprecipitation method with a mass ratio of Fe_3O_4:ZnO of 1:4 with methylene blue degradation efficiency of 97.9% [18]

The difference in synthesis methods has greatly influences photocatalytic activity. The sonochemical method is applied as an environmentally friendly synthesis method, obtaining nanoscale particle sizes with a high yield of nanocomposites. The principle of the sonochemical method utilizes ultrasonic waves that are radiated into the solution. A collision between particles will occur in a crystal breakdown process that allows ZnO-Fe_3O_4 to be nanoscale [19]. The sonochemical method is considered as environmentally friendly because the synthesis process can use ethanol solvents so as not to leave residual waste of dissolution because ethanol will immediately evaporate in the drying process [20].

Consequently, this study aims to synthesize ZnO-Fe_3O_4 magnetic nanocomposites through the sonochemical method. The resulting ZnO-Fe_3O_4 magnetic nanocomposites are characterized and applied in degrading methylene blue under halogen lamp irradiation.

2. Materials and Methods

2.1 Material

The materials used in this study included dried yellow pumpkin seeds (Cucurbita Moschata.), zinc acetate dihydrate ($Zn(CH_3COO)_2.2H_2O$) (Merck), NaOH grade emsure (Merck), ferrous sulfate $FeSO_4.7H_2O$ (Merck), iron(III) chloride hexahydrate $FeCl_3.6H_2O$ (Merck), H_2O_2 grade emplura (Merck), CH_3OH grade emsure (Merck), and methyl blue (Merck).

2.2 Biosynthesis of ZnO Nanoparticles

Yellow pumpkin extract of 10 mL was reacted with $Zn(CH_3COO)_2.2H_2O$ 0.15 M for as much as 90 mL. Then, the mixture was heated at 70 °C for 1 hour in an aqueous bath system while magnetically stirring at 4000 rpm. Furthermore, NaOH 0.1 M was added until the pH of the solution becomes 8, and the sol-gel of ZnO nanoparticles was formed. Next, the formed white sol-gel was separated from the solution by centrifugation at room temperature at 4000 rpm for 10 minutes. Then the precipitate was washed with distilled water and dried at 100 °C for 18 hours. Finally, ZnO precipitate was calcined at 450 °C for 4 hours.

2.3 Synthesis of Fe_3O_4 Magnetic Nanoparticles

A solution of $FeCl_3.6H_2O$ and $FeSO_4.7H_2O$ mixture in a ratio of 2:1 (w/w) was stirred for 30 minutes. Next, 100 mL of 10% NaOH (w/v) was added to the mixture while stirring at 600 rpm for 4 hours at 60 °C. Finally, the formed precipitate was separated using a magnetic field, washed with deionized water until pH = 7, and dried at 60 °C for 8 hours.

2.4 Synthesis of ZnO-Fe_3O_4 Magnetic Nanocomposites

ZnO and Fe_3O_4 (4:1, 5:1, and 6:1 w/w) were transferred into the Erlenmeyer flask and added to as much as 100 mL of ethanol. Then, the mixture was stirred using a magnetic stirrer at

300 rpm for 24 hours at room temperature. Next, the mixture is ultrasonicated for 3 hours and heated at 60 °C overnight. Furthermore, the precipitate was calcined at 300 °C for 2 hours.

2.5 Characterization of ZnO-Fe_3O_4 Magnetic Nanocomposites

The resulting ZnO-Fe_3O_4 magnetic nanocomposites was characterized using XRD (Rigaku Miniflex) to determine their diffraction patterns using Monochromatic Radiation Cu-Kα (λ= 1.54056 Å). Crystallinity, phase type, and sample size were determined by processing XRD diffractogram data using the Match! 3.0 application. The crystal size was determined by the Debye Scherrer equation shown in Equation 1. The ZnO-Fe_3O_4 magnetic nanocomposites morphology also analyzed using an FEI Quanta 650 scanning electron microscope with a 25 kV.

$$D = \frac{k\lambda}{\beta \cos \theta} \quad (1)$$

where, D is crystal size, k is factor of the crystal (0.9), λ is wavelength of X-rays (1.54056 Å), β is full width at half maximum (FWHM) (rad), and θ is angle of diffraction (°).

2.6 Photocatalytic Activity of ZnO-Fe_3O_4 Magnetic Nanocomposites

ZnO-Fe_3O_4 magnetic nanocomposites was dispersed into 100 mL methylene blue solution and stirred at 300 rpm at room temperature. Furthermore, the suspension was irradiated for 3 hours and sampled by 2 mL every 30 minutes. Finally, the suspension was centrifuged at 6000 rpm for 30 minutes. The methylene blue concentration was measured using a UV-Vis spectrophotometer at wavelength 665. The methylene blue degradation efficiency and degradation capacity were calculated using Equations (2)-(3). The dark condition also was measured as a control.

$$DE(\%) = \frac{(C_0 - C_t)}{C_0} x100\% \quad (2)$$

$$DC(mg/g) = \frac{(C_0 - C_t)}{C_0} x \frac{V}{m} \quad (3)$$

where, DE is degradation efficiency (%), DC ((mg/g)) is degradation capacity of methylen blue (mg) per gram ZnO-Fe_3O_4, C_o is initial MB concentration (mg/L), C_t is MB concentration at a certain reaction time (mg/L), V is volume of solution (L), m is ZnO-Fe_3O_4 dosage (g).

The initial methylene blue concentrations (25; 50; 75; and 100 ppm), photocatalyst dosage (25, 50, 75, 100, and 125 mg), pH of the solution (pH = 3, 5, 7, 9, 11, and 13), as well as measurements of the influence of the addition of H_2O_2, CH_3OH, and tert-butanol was observed to determine the optimum condition and species that played a dominant role in the degradation process of methylene blue.

2.7 Stability Analysis of ZnO-Fe_3O_4 Magnetic Nanocomposites

The ZnO-Fe_3O_4 magnetic nanocomposite stability test was performed by measuring the degradation capacity of methylene blue in 10 cycles. After being used, the ZnO-Fe_3O_4 photocatalysts were separated, dried, and analyzed using XRD to confirm their crystal structure stability.

3. Results and Discussion

3.1 Nanoparticles ZnO

The forming of ZnO nanoparticles was carried out using the sol-gel method through the reaction between $Zn(CH_3COO)_2.2H_2O$ as a precursor, yellow pumpkin seed extract (Cucurbita moschata) as a capping agent and reducing agent, and NaOH as a reducing agent. The synthesis of ZnO nanoparticles occurred at pH 8 because pH 8 is a stable condition for making ZnO nanoparticles with the particle size of ZnO produced less than 35 nm. It was reinforced by Saridewi *et al.* who reported that the optimum pH to obtain the smallest ZnO nanoparticles size was pH 8. Since the pH is less or more than 8, there was aggregation on the particle surface which caused the particle size to be larger [21]. The mechanism of the reaction process and the formation of ZnO nanoparticles as a whole can be seen in Figure 1.

Figure 1 explains that the compounds containing hydroxyl and carboxyl groups in yellow

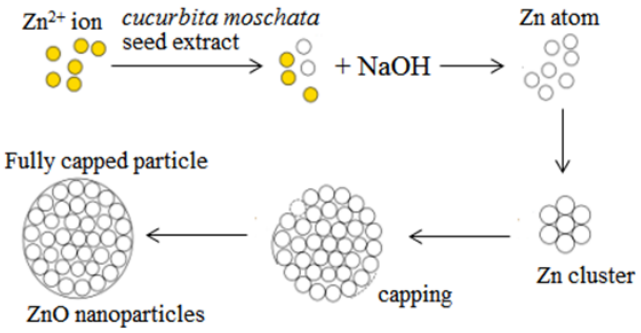

Figure 1. Mechanism of ZnO nanoparticles forming [23]

pumpkin seed extract with NaOH will reduce Zn^{2+} to Zn. Then, the Zn atoms formed merge into Zn clusters. The functional groups in pumpkin seed extract interact with the zinc surface and envelop the Zn cluster, commonly called "capping." A capping agent is an ionic or molecular species that bind to nanoparticles due to the formation of strong covalent bonds between polymer chains and the surface of nanoparticles [23]. Diluting the Zn cluster with a capping agent prevents aggregation between Zn clusters and form stable nanoparticles. The hydroxyl group negatively charged from the compounds in the yellow pumpkin seed extract plays a role in binding to the Zn cluster so that negatively charged ions envelop the particle surface. These negative ions produce a repulsive force between similar charges to prevent nanoparticle aggregation [24].

3.1 ZnO-Fe_3O_4 Magnetic Nanocomposites

Previous study reported that the ZnO-Fe_3O_4 magnetic nanocomposites can be constructed by the sonochemical method. Bhavase *et al.* synthesized Chitosan-ZnO-Fe_3O_4 nanocomposites using the sonochemical method resulting in particle size of 20-40 nm [25]. Manoharan *et al.* also synthesized ZnO/TiO_2/SiO_2 nanocomposites using the sonochemical method with a particle size of 46 nm [26]. Figure 2 shows the ZnO-Fe_3O_4 nanocomposites made with 3 different mass ratios of ZnO and Fe_3O_4, namely (4:1), (5:1), and (6:1), having brown colour with different colour concentrations. If much Fe_3O_4 is added, the brown colour was more intense, because the colour is influenced by the presence of Fe_3O_4, which is deep black.

3.2 ZnO-Fe_3O_4 Magnetic Nanocomposites Crystallinity

Figure 3 shows the diffraction pattern of the three ZnO-Fe_3O_4 magnetic nanocomposites and confirms the phase of the formed crystals. All ZnO-Fe_3O_4 nanocomposites (4:1, 5:1, and 6:1) have the same diffraction peak with a high crystallinity judging from the high spectrum of sharp peaks. The sharp peak of ZnO appears at 2θ is 31.741°; 34.377°; 36.217°; 47.479°; 56.543°; 62.855°; 66.44°; 67.946°; and 69.070° in accordance with JCPDS ZnO no 01-088-0315 (Table 3a). The peak of Fe_3O_4 is also seen at 2θ is 31.42°; 35.51°; 46.98°; 57.04°; and 62.87° following JCPDS Fe_3O_4 no 01-076-0704 (Table 3a).

Figure 3b shows that all magnetic nanocomposites have a larger diffraction pattern towards ZnO with a hexagonal crystalline phase. Because the composition of ZnO is higher than Fe_3O_4, this is also strengthened by Manoharan and coworkers which reporting that reporting nanocomposites ZnO/TiO_2/SiO_2 made with the composition (6:3:1) forming a hexagonal phase with wurtzite morphology [26]. Figure 3b shows that the variation in the addition of Fe_3O_4 does not affect the resulting crystal phase. The crystal size of three ZnO-Fe_3O_4 magnetic nanocomposites is shown in Table 1.

3.3 Morphology of ZnO-Fe_3O_4 Magnetic Nanocomposites

Characterization of scanning electron microscope (SEM) testing was carried out to determine the morphology of the surface of the ZnO-

Table 1. Crystal size of ZnO-Fe_3O_4 magnetic nanocomposites

No	Sample	FWHM	Crystal Size (nm)
1	4:1	0.269	31.058
2	5:1	0.233	35.864
3	6:1	0.458	18.243

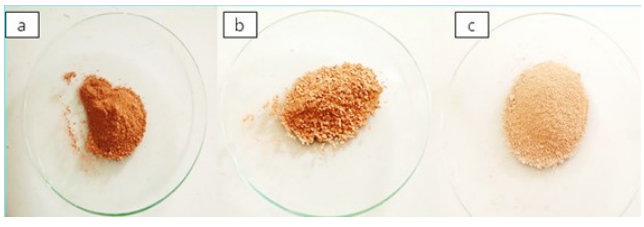

Figure 2. The magnetic nanocomposite ZnO-Fe_3O_4 (a) 4:1, (b) 5:1, and (c) 6:1

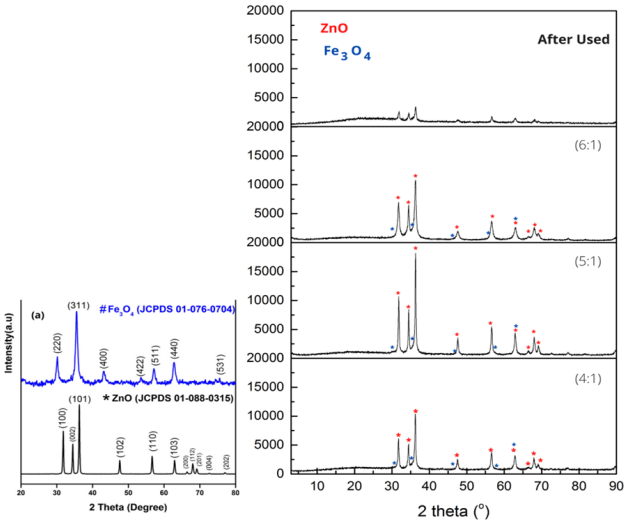

Figure 3. Diffraction patterns (a) JCPDS ZnO and Fe_3O_4, (b) ZnO-Fe_3O_4 magnetic nanocomposites

Fe_3O_4 (4:1). Figure 4 showed that the ZnO-Fe_3O_4 (4:1) magnetic nanocomposite has a spherical morphology with a hexagonal structure. The morphology showed that most of the observed particles are ZnO particles. It is because, in composition (4:1), ZnO has a higher ratio. The morphology was confirmed by Liu *et al.* who reported that composites of ZnO-Fe_3O_4 have a spherical shape and hexagonal structure with the composition of ZnO-Fe_3O_4 (10:7) [26]. In another study, Manoharan also *et al.* reported that ZnO/TiO_2/SiO_2 nanocomposites made with a composition (6:3:1) had a hexagonal phase with wurtzite morphology [27]. Figure 4 also shows the presence of large chunks of particles. These large particles are molecules that do not undergo the process of collision between particles in the sonochemical process, and it is possible that mixing particles is not comprehensive.

Figure 5 exhibits the particle size distribution of ZnO-Fe_3O_4 magnetic nanocomposites using Image-J and Origin softwares. The particle size of the ZnO-Fe_3O_4 nanocomposite is between 150- 200 nm, with an average particle diameter of 173.23 nm. According to Vasquez *et al.*, particles with a diameter size of less than 1000 nm can be considered as nano-size carriers, thus the particle size of the ZnO-Fe_3O_4 magnetic nanocomposites with a diameter of 173.23 nm is nano-sized [28]. The particle size results also did not differ much in Habibi & Shekofteh's research that Fe_3O_4/ZnO/$NiWO_4$ nanocomposites using the sonochemical method produced a particle size of 150 nm [19]. On the other hand, Bykova *et al.* reported that ZnO-Fe_3O_4 synthesized through the solid state method resulted in a particle size of 215.48 nm [29]. In addition, Ghanbarnezhad *et al.* synthesized RGO/Fe_3O_4-ZnO nanocomposites through the hydrothermal method resulted in particle size of 568.23 nm [16]. Wang *et al.* reported that Fe_3O_4@ZnO synthesized through the hydrothermal method resulted in particle size of 220 nm [29].

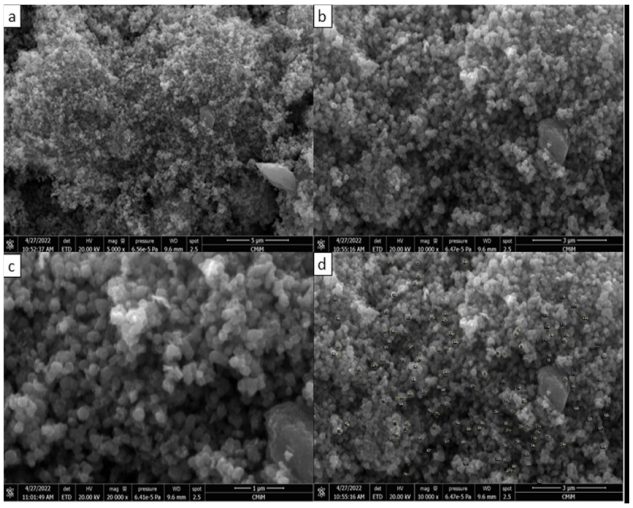

Figure 4. Morphology of ZnO-Fe_3O_4 magnetic nanocomposites (a) magnification of 5000x (b) magnification of 10,000x (c) magnification of 20,000x (d) measurement of particles with Image-J software

3.4 Photocatalytic Activity of ZnO-Fe_3O_4 against Degradation of Methylene Blue

The dark test was carried out to determine the adsorption ability of ZnO-Fe_3O_4 magnetic nanocomposites in methylene blue degradation. Figure 6 showed that all ZnO-Fe_3O_4 magnetic nanocomposites did not show the methylene blue adsorption process under dark conditions. Since both ZnO and Fe_3O_4 have large pore sizes and a small surface area, hence ZnO-Fe_3O_4 provides low ability to adsorb methylene blue. Inline with Elshypany *et al.* study, Fe_3O_4/ZnO nanocomposites had no degradation

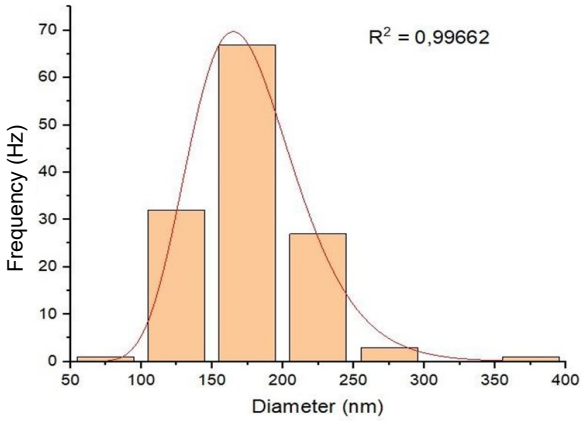

Figure 5. Particle size distribution ZnO-Fe_3O_4 magnetic (4:1)

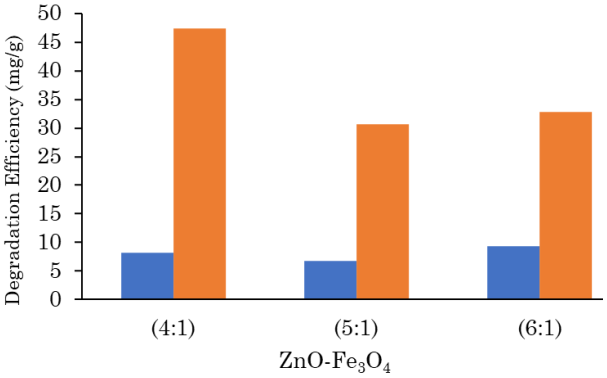

Figure 6. Degradation efficiency of methylene blue by Zn-Fe_3O_4 magnetic nanocomposite in the dark (blue) and light (red) condition

activity in dark conditions because both metals had a large pore size [18]. Seetawan *et al.* also found that the pore size of ZnO in the synthesis using the sonochemical method was 95.3 nm [31]. Shang and Barnabé reported that the pore size of ZnO that is not composted with zeolite is 13.43 nm [32]. Likewise, Rahmawati & Nita studied that the size of the magnetic pore synthesized from natural rocks was 83.74 nm [33]. Each metals has a large pore size, so they tend not to have good activity in adsorbing methylene blue in dark conditions.

Figure 6 shows that ZnO-Fe_3O_4 (4:1) degrades methylene blue by 47.36% in light conditions. Under light conditions, the photon energy from the halogen lamp hits the ZnO-Fe_3O_4 photocatalyst. Then, it forms hydroxyl radical (OH^*) for the photodegradation of methyl blue [34]. Figure 6 shows that the nanocomposites at ZnO:Fe_3O_4 (4:1) gave the largest degradation efficiency of 47.36%. ZnO nanoparticles play the main role as photocatalysts [9-11], while Fe_3O_4 contributes to separate photocatalyst particles. Therefore, photocatalysts continuously undergo degradation [12]. It is also related to comparing the composition of the used nanoparticles. When more ZnO ratio was used, nanocomposites' photocatalytic degradation activity decreases because of the colloidal system formation, and the less magnetic properties, and the strength in attracting photocatalysts decreases [35]. The magnetic properties ZnO-Fe_3O_4 (6:1) is smaller than (5:1), as well as (5:1) the magnetic content is smaller than (4:1). Therefore, the methylene blue degradation by ZnO-Fe_3O_4 (4:1)>(5:1)>(6:1). The mechanism of photocatalytic degradation of methylene blue by ZnO-Fe_3O_4 is shown in Figure 7.

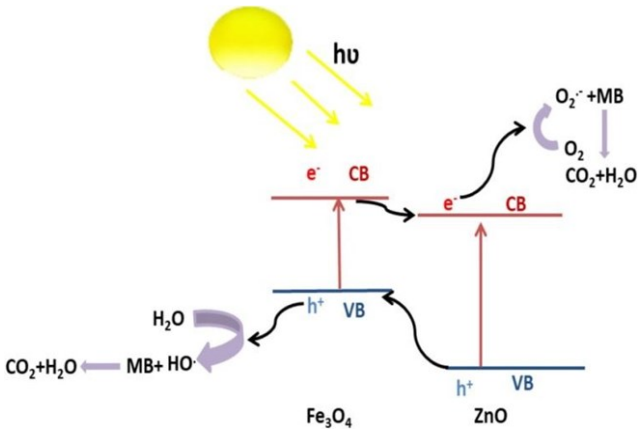

Figure 7. Photocatalytic degradation mechanism of methylene blue by ZnO-Fe_3O_4 magnetic nanocomposite [34]

3.5 Effect of Methylene Blue Concentration

The optimum condition of ZnO-Fe_3O_4 magnetic nanocomposites in degrading methylene blue is at 50 ppm with a degradation capacity of 31.51 mg/gram. Figure 8 shows no photocatalytic degradation at an MB concentration of 100 ppm. It is due to the photocatalyst being in the saturated phase due to the high concentration of dyes covering the surface of the photocatalyst. The saturated photocatalysts decreases photon efficiency and improve photocatalyst deactivation [36]. Zhang *et al.* reported that adding methyl orange concentrations from 5 ppm to 10 ppm in ZnO-TiO_2 nanocomposites could provide an ever-increasing degradation capacity. However, adding 25 ppm concentration decreases the degradation [37].

3.6 Effect of ZnO-Fe_3O_4 Magnetic Nanocomposite Dosage

Figure 9 revealed that the optimum photocatalyst dosage is 25 mg with a degradation ca-

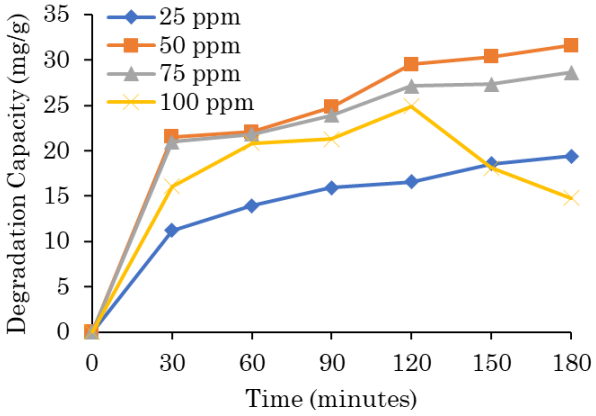

Figure 8. Degradation capacity of methylene blue by ZnO-Fe_3O_4 magnetic nanocomposites at variations in methylene blue concentrations

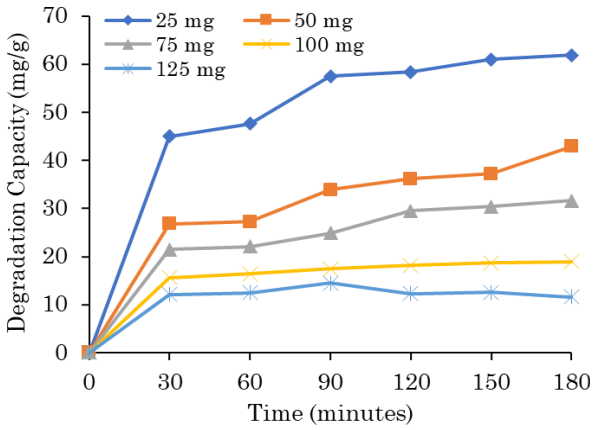

Figure 9. Degradation capacity of methylene blue by ZnO-Fe_3O_4 magnetic nanocomposites on any photocatalyst dosage

pacity of 61.87 mg/g. Nevertheless, a photocatalyst dosage of 25 mg cannot be separated externally because the photocatalyst is perfectly dispersed in the solution making it difficult to separate. It can not be considered an optimum condition because photocatalysts can only be used once due to the difficulty of the separation process after use. A photocatalyst dosage of 50 mg is optimal because a photocatalyst dosage of 50 mg provides the highest degradation capacity of 42.85 mg/g and is easy to separate using external magnets.

Figure 9 also shows that the increased in the photocatalysts' dosage affects their photocatalytic activity in degrading methylene blue. However, if the photocatalysts dosage is used too much, it decreases the degradation capacity. Kumar & Pandey explained that the more photocatalyst dosages used cause the active sites where the reaction occurs to be more numerous [38]. Then, too many photocatalysts also affect the turbidity of the solution. As a result, a cloudy solution makes it difficult for a beam to reach the photocatalyst's active site, causing the photocatalyst's surface to become obstructed, resulting in a decrease in the percentage of degradation [38].

3.7 Effect of pH

Figure 10 shows optimum conditions resulting in a degradation capacity of 99.44 mg/gram at pH of 13, then 91.58 mg/gram at pH of 11, and 42.85 mg/gram at pH of 9. The neutral pH was also degraded by 30.06 mg/gram. Meanwhile, acidic conditions, namely pH of 3 and 5 degradation results, tend to be subdued. In acidic conditions, ZnO tends to be positively charged because ZnO interacts more with ion H^+, whereas the blue methylene in the solution is also positively charged. This reaction between positive charges tends to be less preferred, which causes less than optimum percentage degradation [38].

On the other hand, in alkaline conditions, ZnO is negatively charged, so it is preferred to react with positively charged methylene blue [39]. The methylene blue is a cationic dye (positively charged), so the alkaline pH increases the effectiveness of photodegradation because an increase in OH ions increases the amount of OH radicals produced. The acid and base pH reaction at ZnO is shown in Equations (3)-(4).

$$(PH < 6.8) : Zn\text{-}OH + H^+ \rightarrow ZnOH_2^+ \quad (3)$$

$$(PH > 6.8) : Zn\text{-}OH + OH^- \rightarrow ZnO^- + H_2O \quad (4)$$

3.8 Dominant Species on Photocatalytic Activity of Methylene Blue

Figure 11 shows that adding of H_2O_2, resulting in a degradation capacity of 99.80 mg/gram for 30 min. Then the addition the mixture of the tertiary butanol (tert-BuOH) and H_2O_2 resulted in a degradation capacity of 99.29 mg/gram simultaneously. Finally, adding methanol resulted in a degradation capacity of 78.08 mg/gram. Meanwhile, a degradation capacity of 88.43 mg/gram without adding sacrificial agents was obtained. Thus, adding H_2O_2 contributes greatly to the photodegradation reaction of methylene blue. In addition, the H_2O_2 added to the system will capture photogenerated electrons to prevent recombination between the photogenerated electron and the electron-hole pairs [40].

In addition, H_2O_2 also reacts with photogenerated electrons producing radicals (OH^*) and hydroxides (OH^-) [41]. Electron holes in the valence band in the ZnO-Fe_3O_4 magnetic nano-

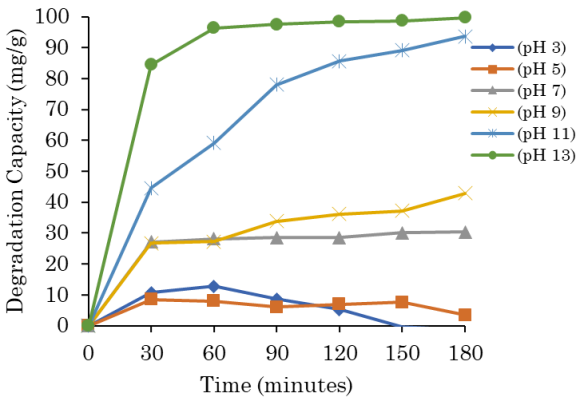

Figure 10. Degradation capacity of methylene blue by ZnO-Fe_3O_4 magnetic nanocomposite at pH variations

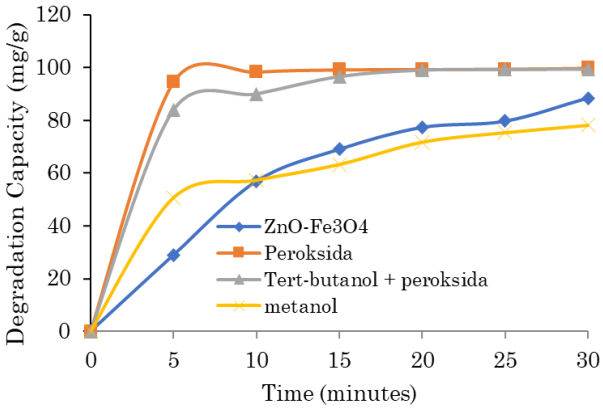

Figure 11. Degradation capacity of methylene blue by ZnO-Fe_3O_4 magnetic nanocomposite on variations in the addition of sacrificial agents

composite skeleton is stabilized through reactions with water forming hydroxyl radicals (OH^*). On the other hand, H_2O_2 can also be decomposed by light-producing hydroxyl radicals (OH^*), so it plays the most important role in photocatalytic reactions of methylene blue degradation. The mechanism is written in Equations (5)-(11).

$$ZnO\text{-}Fe_3O_4 + h\upsilon \rightarrow ZnO\text{-}Fe_3O_4\ (e^-_{cb}) + ZnO\text{-}Fe_3O_4\ (h^+_{vb}) \quad (5)$$

$$ZnO\text{-}Fe_3O_4\ (e^-_{cb}) + H_2O_2 \rightarrow OH^* + OH^- \quad (6)$$

$$H_2O_2 + h\upsilon \rightarrow 2OH^* \quad (7)$$

$$ZnO\text{-}Fe_3O_4\ (h^+_{vb}) + OH^- \rightarrow OH^* \quad (8)$$

$$ZnO\text{-}Fe_3O_4\ (h^+_{vb}) + H_2O \rightarrow OH^* + H^+ \quad (9)$$

$$(CH_3)_3COH + OH^* \rightarrow H_2O + (CH_3)CO^- \quad (10)$$

$$OH^* + MB \rightarrow \text{degradation products} \quad (11)$$

The addition of tert-BuOH and H_2O_2 provided a slightly decreasing photocatalytic activity of methylene blue degradation of 99.29 mg/gram at 30 minutes of reaction time. It is because tert-BuOH captures hydroxyl radicals, which decreases the number of hydroxyl radicals and decreases the efficiency of methylene blue degradation. The methanol added to the system will capture electron holes (h^+) and oxidize methanol to hydroxyalkyl radicals (CH_2OH^*) and oxidize further to formaldehyde (CH_2O). Thus, there are no hydroxyl radicals (OH^*) formation, which plays an important role in the MB photodegradation process. Instead, photogenerated electrons will react with oxygen absorbed on the surface of $ZnO\text{-}Fe_3O_4$ to form a superoxide radical (O_2^{-*}), where the radical will also react with methylene blue to form a degradation product. The mechanism is written in Equations (12)-(15).

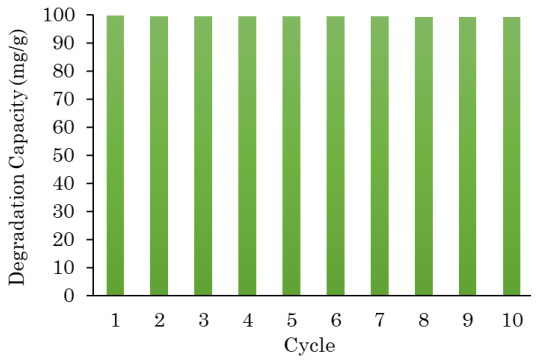

Figure 12. Methylene blue degradation efficiency by $ZnO\text{-}Fe_3O_4$ nanocomposites in 10 times the reaction cycle

$$ZnO\text{-}Fe_3O_4\ (h^+_{vb}) + CH_3OH \rightarrow CH_3OH^* \quad (12)$$

$$CH_3OH^* \rightarrow CH_2O + H^+ + e^- \quad (13)$$

$$ZnO\text{-}Fe_3O_4\ (e^-_{cb}) + O_2 \rightarrow O_2^{-*} \quad (14)$$

$$O_2^{-*} + MB \rightarrow \text{degradation products} \quad (15)$$

3.9 Stability of $ZnO\text{-}Fe_3O_4$ Magnetic Nanocomposite

Figure 12 exhibited that $ZnO\text{-}Fe_3O_4$ (4:1) magnetic nanocomposite has good stability after 10 cycles. It produces a methylene blue degradation capacity of approximately 99.75–99.24%. This result is much better compared to other studies, i.e. Elshypany *et al*. synthesized Fe_3O_4/ZnO magnetic nanocomposite with a degradation efficiency of 88.5% for 5 cycles [18]. Dehghan *et al*. also reported that $ZnO\text{-}Fe_3O_4$ nanocomposites that stable for as many as 5 cycles with a degradation efficiency of 90%-85% [42]. Adding Fe_3O_4 to ZnO magnetic nanoparticle can separate ZnO photocatalysts, so that ZnO can be used simultaneously. The $ZnO\text{-}Fe_3O_4$ stability was also confirmed by no changes in the diffraction pattern of $ZnO\text{-}Fe_3O_4$ nanocomposites before and after use (Figure 3b).

4. Conclusion

The $ZnO\text{-}Fe_3O_4$ magnetic nanocomposite was made by sonochemical method with a mass ratio of ZnO and Fe_3O_4 (4:1 b/b), resulted in the most optimal methylene blue degradation, having a crystal size of 31.058 nm and a particle size of 173.23 nm with a hexagonal crystal phase. In addition, $ZnO\text{-}Fe_3O_4$ magnetic nanocomposite (4:1) has good stability after use for 10 reaction cycles with a degradation capacity of about 99.75-99.24 mg/gram at pH 13 under halogen lamp irradiation for 180 minutes.

Acknowledgement

The authors would like to thank UIN Syarif Hidayatullah Jakarta for financial support with the contract number B-304/LP2M-PUSLITPEN/TL.03/2022. In addition, thanks to Universitas Indonesia for facilitating to carrying out of this work.

References

[1] Gürses, A., Hassani, A., Kranşan, M., Açşl, Ö., Karaca, S. (2014). Removal of methylene blue from aqueous solution using by untreated lignite as potential low-cost adsorbent: kinetic, thermodynamic and equilibrium approach. *Journal of Water Process Engineering*, 2(1), 10–21. DOI: 10.1016/j.jwpe.2014.03.002

[2] Choi, H.J., Yu, S.W. (2019). Biosorption of methylene blue from aqueous solution by agricultural bioadsorbent corncob. *Environmental Engineering Research*, 24(1), 99–106. DOI: 10.4491/eer.2018.107

[3] Sakti, R.B., Subagio, A., Susanto, H. (2013). Synthesis of thin layers of TiO_2/CNT nanocomposites using sol-gel method and their application to photodegradation of dyestuffs azo orange 3R. *Youngster Physics Journal*, 2(2), 41–48.

[4] Sistesya, D., Sutanto, H. (2013). Optical properties of ZnO:Ag coatings deposited over glass substrates using the chemical deposition (CSD) method and their application to the degradation of methylene blue dyestuffs. *Youngster Physics Journal*, 1(4), 71–80.

[5] Ivanova, T., Harizanova, A., Koutzarova, T., Vertruyen, B. (2011). Preparation and characterization of ZnO-TiO_2 films obtained by sol-gel method. *Journal of Non-Crystalline Solids*, 357(15), 2840–2845. DOI: 10.1016/j.jnoncrysol.2011.03.019

[6] Pant, H.M., Bishweshwar, P., Ram, K.S., Amarjagal, A., Kim, H.J., Chan, Park, C.H., Tijing, L.D., Kim, C.S. (2013). Antibacterial and photocatalytic properties of Ag/TiO_2/ZnO nano-flowers prepared by facile one-pot hydrothermal process. *Ceramics International*, 39 (2), 1503–1510. DOI: 10.1016/j.ceramint.2012.07.097

[7] Xu, L., Zheng, G., Wu, H., Wang, J., Gu, F., Su, J., Xian, F., Liu, Z. (2013). Strong ultraviolet and violet emissions from ZnO/TiO_2 multilayer thin films. *Optical Materials*, *35*, 1582–1586. DOI: 10.1016/j.optmat.2013.04.001

[8] Raganata, T.C., Aritonang, H., Suryanto, E. (2019). Photocatalyst synthesis of ZnO nanoparticles to degrade methlene blue dyestuffs. *Chem Prog*, 12(2), 55–58. DOI: 10.35799/cp.12.2.2019.27923

[9] Oliviera, L.C.A., Fabris, J.D., Perreira, M.C. (2013). Iron oxides and their applications in catalytic processes: A review. *Química Nova*, 36(1), 123–130. DOI: 10.1590/S0100-40422013000100022

[10] Nikitin, A., Fedorova, M., Naumenko, V. Shchetinin, I., Abakumov, M, Erofeev, A., Gorelkin, P., Meskov, G., Beloglazkina, E., Ivanenkov, Y., Klyachko, N., Golovin, Y., Savchenko A., Majouga, A. (2017). Synthesis, characterization and MRI application of magnetite water-soluble cubic nanoparticles. *Journal of Magnetism and Magnetic Materials*, 441, 6–13. DOI: 10.1016/j.jmmm.2017.05.039

[11] Zhang, H., Guo, L., Ding, S., Xiong, J., Chen, B. (2016). Targeted photo-chemo therapy of malignancy on the chestwall while cardiopulmonary avoidance based on Fe_3O_4@ZnO nanocomposites. *Oncotarget*, 7(24), 36602–36613. DOI: 10.18632/oncotarget.9123

[12] Bilalodin, B., Sunardi, S., Effendy, M. (2013). Chemical compound content analysis and magnetic properties test of ambal beach iron sand. *Indonesian Journal of Physics*, 17(50), 29–31. DOI: 10.22146/jfi.24420

[13] Ulya, H.N., Taufiq, A. Sunaryo, S. (2019). comparative structural properties of nanosized ZnO/Fe_3O_4 composites prepared by sonochemical and sol-gel methods comparative structural properties of nanosized ZnO/Fe_3O_4 composites prepared by sonochemical and sol-gel methods. *IOP Conf. Ser.: Earth Environ. Sci*. 276 012059, DOI: 10.1088/1755-1315/276/1/012059

[14] Yogasundari, M., Manikandan, A. (2020). Synthesis, structural, morphological and mabnetic properties of Fe_3O_4/ZnO nanocomposites by co-precipitation method. *Malaya Journal of Matematik*, 1(2), 2264–2266. DOI: 10.1016/j.physe.2020.114291

[15] Ghanbarnezhad, S., Baghshahi, S., Nemati, A., Mahmoodi, M. (2017). Preparation, magnetic properties, and photocatalytic performance under natural daylight irradiation of Fe_3O_4-ZnO core/shell nanoparticles designed on reduced GO platelet. *Materials Science in Semiconductor Processing*, 72, 85–92. DOI: 10.1016/j.mssp.2017.09.015

[16] Winatapura, D.S., Dewi, S.H., Adi, W.A. (2016). Synthesis, characterization, and photocatalytic activity of Fe_3O_4@ZnO nanocomposite. *International Journal of Technology*, 7(3), 408–416. DOI: 10.14716/ijtech.v7i3.2952

[17] Elshypany, R., Selim, H., Zakaria, K., Moustafa, A.H., Sadeek, A.S., Sharaa, S.., Raynaud, P., Nada, A.A. (2021). Elaboration of Fe_3O_4/ZnO nanocomposite with highly perfome photocatalytic activity for degradation methylene blue under visible light irradiation. *Environmental Technology & Inovation*, 23, 101710. DOI: 10.1016/j.eti.2021.101710

[18] Yangjeh A.H., Maryam, S.G. (2017). Novel magnetic Fe_3O_4/ZnO/$NiWO_4$ nanocomposites : enhanced visible-light photocatalytic perfomance through p-n heterojunctions. *Separation and Purification Technology*, 184, 334–346. DOI: 10.1016/j.seppur.2017.05.007

[19] Kusuma, S.W.N. (2016). *Inorganic Synthesis*. Padang : UNP Press Padang.

[20] Toprakci, O., Toprakci, H.A.K., Liwen, J., Xiangwu, Z. (2010). Fabrication and electrochemical characteristics of $LiFePO_4$ powders for lithium-ion batteries. *KONA Powder and x Particle Journal*, 28(28), 50–73. DOI: 10.14356/kona.2010008

[21] Saridewi, N., Syaputro, H.T., Aziz, I., Dasumiati, D., Kumila, B.N. (2021). Synthesis and characterization of ZnO nanoparticles using pumpkin seed extract (Cucurbita moschata) by the sol-gel method. *4th International Seminar on Chemistry*, 2349(June), 020010. DOI: 10.1063/5.0051826

[22] Mollahosseini, A., Toghroli, M. (2015). Synthesis and identification of Fe_3O_4/clinoptilolite magnetic nanocomposite. *Journal of Asian Scientific Research*, 5(3), 120–125. DOI: 10.18488/journal.2/2015.5.3/2.3.120.125

[23] Nurbayasari, R., Saridewi, N., iShofwatunnisa, S. (2017). Biosynthesis and characterization of ZnO nanoparticles with extract of green seaweed sp. *Jurnal Perikanan Universitas Gadjah Mada*, 19(1), 17–28. DOI: 10.22146/jfs.24488

[24] Tournebize, J., Boudier, A., Joubert, O., Eidi, H., Bartosz, G., Maincent, P., Leroy, P., Minet A.S. (2012). Impact of gold nanoparticle coating on redox homeostasis. *International Journal of Pharmaceutics*, 438, 107–116. DOI: 10.1016/j.ijpharm.2012.07.026

[25] Bhavase, B., Veer, A., Shirsath, S., Sonowane, S,H. (2019). ultrasound assisted preparation, characterization and adsorption study of ternary chitosan-ZnO-TiO_2 nanocomposite: advantage over conventional method. *Ultrasonics Sonochemistry*, 52, 120–130. DOI: 10.1016/j.ultsonch.2018.11.003

[26] Liu, Q., Zhou, L., Liu, L., Li, J., Shaobin, W., Hussein, Z., Liu, S. (2020). Magnetic ZnO@Fe_3O_4 composite for self-generated H_2O_2 toward photo-fenton-like oxidation of nitrophenol. *Composites Part B 200*, 108345, 1–8. DOI: 10.1016/j.compositesb.2020.108345

[27] Manoharan, C., Rajendran, V., Sivaraj, R. (2018). Synthesis, characterization and applications of ZnO/TiO_2/SiO_2 zinc (tris) thiourea sulfate nanocomposite. *Orient Journal of Chemistry*, 34(3), 1333–1340. DOI: 10.13005/ojc/340319

[28] Vasquez, R.D., Apostol, J.G, de Leon J.D., Mariano, J.D., Mirhan, C.M.C., Pangan,S.S., Reyes, A.G.M., Zamora, E.T. (2016). Polysaccharide-mediated green synthesis of silver nanoparticles from sargassum siliqousum: Assessment of toxicity activity. *Open Nano*, 1, 16–24. DOI: 10.1016/j.onano.2016.03.001

[29] Bykova, L.E., Myagov, V.G., Tambasov, I.A., Bayukov, O.A., Zhivalov, V.S., Bondarenko, G.N., Nemtsev, I.V., Polyakova, V.V., Patrin, G.S., Velikanov, D.A. (2015). Solid-state synthesis of the ZnO-Fe_3O_4 nanocomposite: structural and magnetic properties. *Physics of the Solid State*, 57(2), 386–390. DOI: 10.1134/S1063783415020079

[30] Wang, J., Yang, J., Li, X., Wang, D., Wei, B., Song, H., Li, X., Fu, S. (2016). Preparation and photocatalytic properties of magnetically reusable Fe_3O_4@ZnO core/shell nanoparticles. *Physica*, 75(1), 66–71. DOI: 10.1016/j.physe.2015.08.040

[31] Seetawan, U., Jugsujinda, S., Seetawan, T., Ratchasin, A., Euvananont, C., Junin, C., Thanachayanont, C., Chainaronk, P. (2011). Effect of calcinations temperature on crystallography and nanoparticles in ZnO disk. *Materials Sciences and Applications*, 2(9), 1302–1306. DOI: 10.4236/msa.2011.29176

[32] Shang, C., Barnabé, A. (2013). Structural study and phase transition investigation in a simple synthesis of porous architected-ZnO nanopowder. *Materials Characterization*, 86, 206–211. DOI: 10.1016/j.matchar.2013.10.004

[33] Rahmawati, R., Handayani, H. (2013). Ferrogel fabrication based on magnetic nanoparticles (Fe_3O_4) from the synthesis of iron sands on the north coast of java and the properties of magneto elsatis. *Neutrino Journal*, 5(2), 95–104. DOI: 10.18860/neu.v0i0.2437

[34] Natarajan, S., Bajaj, H.C., Tayade, R.J. (2018). Recent advances based on the synergetic effect of adsorption for removal of dyes from waste water using photocatalytic process. *Journal of Environmental Sciences (China)*, 65, 201–222. DOI: 10.1016/j.jes.2017.03.011

[35] Teja, A.S., Yoon, K.P. (2009). Synthesis, properties, and application of magnetic iron oxide nanoparticles. *Progress in Crystal Growth and Characterization of Materials*, 55(1), 22–45. DOI: 10.1016/j.pcrysgrow.2008.08.003

[36] Chen, X., Mao, S.S. (2007). Titanium dioxide nanomaterials: synthesis, properties, modifications and applications. *Chemical Reviews*, 107(7), 2891–2959. DOI: 10.1021/cr0500535

[37] Zhang, M., An, T., Liu, X., Hu, X., Sheng, G., Fu, J. (2010). Preparation of a high-activity ZnO/TiO2 photocatalyst via homogeneous hydrolysis method with low temperature crystallization. *Materials Letters*, 64(17), 1883–1886. DOI: 10.1016/j.matlet.2010.05.054

[38] Kumar, A., Pandey, G. (2017). A review on the factors affecting the photocatalytic degradation of hazardous materials. *Material Science & Engineering International Journal*, 1(3), 106–114. DOI: 10.15406/mseij.2017.01.00018

[39] Lee, B., Jeon, Y., Kwon, J. (2006). Study on pH sensor using methylene blue adsorption and a long-period optical fiber grating pair. *Journal of the Optical Society of Korea*, 10(1), 28–32. DOI: 10.3807/JOSK.2006.10.1.028

[40] Zhang, P., Wang, Y., Zhou, Y., Zhang, H., Wei, X., Sun, W., Meng, S., Han, L. (2019). Preparation and photocatalytic properties of magnetic g-C_3N_4/TNTs nanocomposites. *Molecular Catalysis*, 465, 24–32. DOI: 10.1016/j.mcat.2018.12.023

[41] Zhou, D., Cheng, Z., Yang, Q., Dong, X., Zhang, J., Qin, L. (2016). In situ construction of all solid state Z-scheme g@C3N4/TiO2 nanotube arrays photocatayst with enhanced visible light induced. Solar Energy Meter, 157, 399–405. DOI: 10.1016/j.solmat.2016.07.007

[42] Dehghan, S., Babak, K., Roshanak, R.K. (2018). Heterogeneous sonocatalytic degradation of amoxicillin using ZnO@Fe_3O_4 magnetic nanocomposite: influential factors, reusability and mechanisms. *Journal of Molecular Liquids*, 1–42. DOI: 10.1016/j.molliq.2018.05.020